

Search for or Navigate to? Dual Adaptive Thinking for Object Navigation

Ronghao Dang¹, Liuyi Wang¹, Zongtao He¹, Shuai Su¹, Chengju Liu^{1,2*}, Qijun Chen¹

¹Department of Control Science and Engineering, Tongji University, Shanghai 201804, China

²Tongji Artificial Intelligence (Suzhou) Research Institute, Suzhou 215000, China
{dangronghao, wly, xingchen327, sushuai, liuchengju, qjchen}@tongji.edu.cn

Abstract

“Search for” or “Navigate to”? When finding an object, the two choices always come up in our subconscious mind. Before seeing the target, we search for the target based on experience. After seeing the target, we remember the target location and navigate to. However, recently methods in object navigation field almost only consider using object association to enhance “search for” phase while neglect the importance of “navigate to” phase. Therefore, this paper proposes the dual adaptive thinking (DAT) method to flexibly adjust the different thinking strategies at different navigation stages. Dual thinking includes search thinking with the object association ability and navigation thinking with the target location ability. To make the navigation thinking more effective, we design the target-oriented memory graph (TOMG) to store historical target information and the target-aware multi-scale aggregator (TAMSA) to encode the relative target position. We assess our methods on the AI2-Thor dataset. Compared with the state-of-the-art (SOTA) method, our method reports 10.8%, 21.5% and 15.7% increase in success rate (SR), success weighted by path length (SPL) and success weighted by navigation efficiency (SNE), respectively.

Introduction

Object navigation (Moghaddam et al. 2022; Li et al. 2022) is a challenging task that requires an agent to find a target object in an unknown environment with the first-person visual observation. Due to the limited view field, the information to guide the agent navigation is insufficient. Therefore, some researchers recently introduced scene prior knowledge into the navigation network. Through these methods, the problems of how to use object association (Yang et al. 2019), object attention bias (Dang et al. 2022), and lack of universal knowledge (Gao et al. 2021) are solved. However, these methods only improve the efficiency of “search for” phase (start→first seeing target) but not “navigate to” phase (first seeing target→end). Through our experiments we found that for the current SOTA end-to-end methods, the “navigate to” steps accounts for 60% of the whole path, while only 40% for humans; the success rate after seeing the target is only 80%, while humans can reach 100%.

*Corresponding author

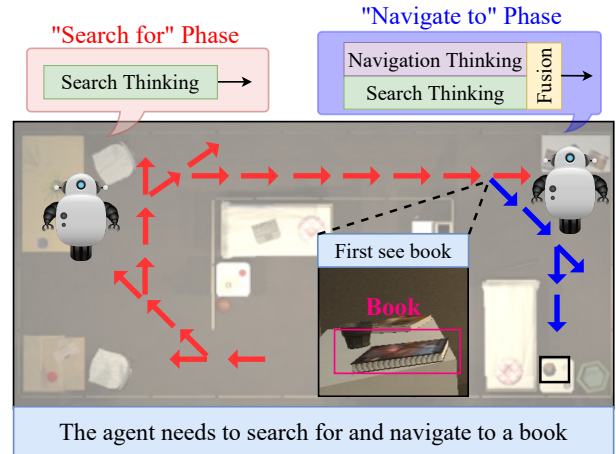


Figure 1: We divide the agent’s navigation process into two phases: “search for” (red) and “navigate to” (blue). During the “search for” phase, the agent only uses the search thinking to search for the target. During the “navigate to” phase, the navigation thinking assists the agent to quickly navigate to the target location.

Some modular approaches (Chaplot et al. 2020; Ramakrishnan et al. 2022) model the environment by using top-down semantic maps. With the help of the detailed semantic maps, the object navigation task can be decoupled into two separate training sub-tasks: predicting the sub-target point and navigating to the sub-target point, thus optimizing the agent navigation ability after seeing the target. However, these methods are strongly dependent on semantic maps which are hypersensitive to the sensory noise and scene changes. Furthermore, high-quality semantic maps need to consume a large number of computational resources.

In order to solve the above problems, we hope to integrate the task decoupling idea from the modular methods into the end-to-end methods. Therefore, we propose the dual adaptive thinking (DAT) method. As shown in Figure 1, The agent’s thinking modes are divided into search thinking and navigation thinking. Search thinking guides the agent to quickly find the target with the help of prior knowledge and object association. Navigation thinking assists the agent

to efficiently navigate to the target position after finding the target. The agent can adaptively adjust the dominance of the two thinking ways in an end-to-end network according to the navigation progress.

Specifically, we have completely different designs for the search thinking network and the navigation thinking network. For the search thinking network, we draw on the DOA graph method in (Dang et al. 2022) to design the object association and attention allocation strategy. For the navigation thinking network, in order to have the memory capability, we use the target-oriented memory graph (TOMG) to store the simplified agent state and target orientation information. Furthermore, we design the target-aware multi-scale aggregator (TAMSA) to refine the features in the TOMG to guide the agent’s navigation.

Extensive experiments on the AI2-Thor (Kolve et al. 2017) dataset show that our dual adaptive thinking (DAT) method not only optimizes the “navigate to” phase in the end-to-end network, but also outperforms the state-of-the-art (SOTA) method (Dang et al. 2022) by 10.8% and 21.5% in the success rate (SR) and success weighted by path length (SPL). We propose a new metric, success weighted by navigation efficiency (SNE), which represents the agent’s navigation ability during the “navigate to” phase. As a general idea, the proposed multiple thinking strategy can inspire many other embodied AI tasks. In summary, our contributions are as follows:

- We propose the dual adaptive thinking (DAT) method that allows the agent to flexibly use different modes of thinking during the navigation.
- We carefully design the navigation thinking network with selective memory module (TOMG) and feature refinement module (TAMSA).
- We demonstrate that our DAT method can not only address the inefficiency in the “navigate to” phase, but also greatly improve the performance of the current object navigation model.

Related Works

Object Navigation

The object navigation task needs an agent to navigate to target objects in an unknown environment with only visual inputs. The primitive works use a simple black-box model to encode visual features into a high-dimensional space, which is then fed directly into the decision model. Recently, the relationships between objects are introduced into the navigation network, so that the agent can find targets through association more quickly. In (Zhang et al. 2021), the hierarchical object-to-zone (HOZ) graph guides an agent in a coarse-to-fine manner. Researchers (Dang et al. 2022) utilize the directed object attention (DOA) graph to solve the object attention bias problem. Although these works enable agents to find targets faster, they do not address the problem of how to navigate to targets quickly.

In order to strengthen the agent’s memory ability, some works enable the agent to memorize the past visual features through external storage. GBE (Zhu et al. 2021) models the

navigation state as a discretized graph and introduces a novel graph-based exploration approach to learn knowledge from the graph. An object memory transformer (OMT) network (Fukushima et al. 2022) are proposed to model the long-term memory of object features. Regrettably, these memory methods still employ a single thinking network with no selective memory. Our dual adaptive thinking (DAT) method divides the thinking into two types: search thinking and navigation thinking, which can switch and collaborate adaptively with the help of the target-oriented memory module.

Modular Navigation

The modular navigation method is proposed to solve the generalization problem of end-to-end models in complex environments. It is proved that using a top-down semantic map to predict distant sub-goal points (Chaplot et al. 2020) is feasible on the Habitat dataset. PONI (Ramakrishnan et al. 2022) method trains two potential function networks using supervised learning to decide where to look for an unseen object. These modular methods all need to spend a large number of computing and storage resources to generate semantic maps in real time which is sensitive to the image segmentation quality. Our method implicitly incorporates different thinking during navigation into an end-to-end network without relying on semantic maps.

Necessity of Dual Thinking

Dual Thinking of Humans

Embodied AI (Duan et al. 2022) is a challenging research which requires an agent to use the currently well-developed intuitive tasks (e.g., classification (Wang et al. 2019) and detection (Liu et al. 2020)) to complete the complex logical tasks (e.g., navigation (Zhu, Meurer, and Günther 2022) and interaction (Shridhar et al. 2020)) in the real world. Humans often do not use only one way of thinking when completing these complex logical tasks. For example, when we need an object, we first use associative thinking to find the object, and then use navigational thinking to reach the object location; when we answer a question about an object, we first use exploratory thinking to fully understand the object, and then use reasoning and language-organized thinking to draw conclusions. Therefore, the introduction of multiple thinking in an end-to-end network can make the model more hierarchical and interpretable, which is in line with the way humans deal with complex logic problems.

Target Repeatedly Search Problem

There is a phenomenon in the current methods that if the agent lost the target in view, it still needs to be searched again to lock the target. This phenomenon causes the agent to waste considerable time in re-searching the target and even leads to a constant loop. After years of development, the current navigation network has a strong ability to associate objects which is only helpful for searching. However, unlike a human, the agent cannot have a clear orientation memory of the target after seeing it. Therefore, we design the target-oriented memory graph (TOMG) and the target-aware multi-scale aggregator (TAMSA) in the navigation thinking

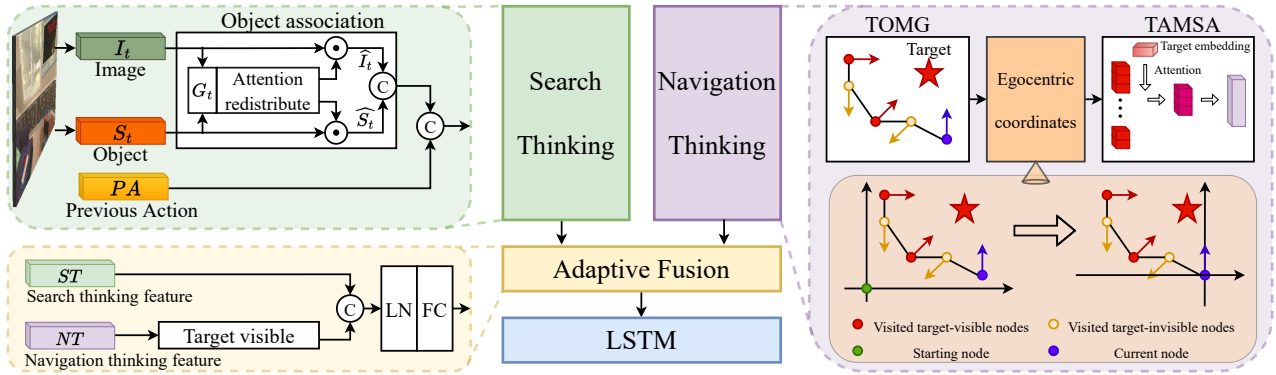


Figure 2: Model overview. TOMG: target-oriented memory graph. TAMSA: target-aware multi-scale aggregator. Our model consists of three modules: search thinking, navigation thinking and adaptive fusion. In the search thinking network, we endow the model with the object association ability according to the DOA graph method in (Dang et al. 2022). In the navigation thinking network, we give the model the ability to remember the target orientation. In the adaptive fusion network, we make the dual thinking work in harmony according to the navigation progress.

network to make the agent efficiently navigate to the target without repeatedly re-searching.

Dual Adaptive Thinking Network

Our goal is to endow agents with both search and navigation thinking, and adjust their work status based on the navigation progress. To achieve this goal, we design three networks, as illustrated in Figure 2: (i) search thinking network; (ii) navigation thinking network; (iii) adaptive fusion network. (i) and (ii) are connected together by (iii) to form a dual adaptive thinking (DAT) network.

Task Definition

In the object navigation task, the agent receives the target object $p \in P = \{Pan, \dots, Cellphone\}$ at the beginning, selects the action a_t according to the RGB image o_t from a single view at each step t , and finally navigates to the target location. Initially, the agent is initialized to a random state $s = \{x, y, \theta, \beta\}$ in a random room. According to o_t and p , the agent learns a navigation strategy $\pi(a_t|o_t, p)$, where $a_t \in A = \{MoveAhead; RotateLeft; RotateRight; LookDown; LookUp; Done\}$ and *Done* is the output if the agent believes it has navigated to the target location. Ultimately, if the agent is within 1.5m of the target object when *Done* is output, the navigation episode is considered successful.

Search Thinking Network

Search thinking aims to enable the agent to quickly capture the target with the fewest steps when there is no target in view. Therefore, we adopt the unbiased directed object attention (DOA) graph method proposed in (Dang et al. 2022). Using the object-target association score G_t calculated by the DOA method, we redistribute the attention to the object features S_t (from DETR (Carion et al. 2020)) and the image features I_t (from ResNet18 (He et al. 2016)) respectively so that the agent pays attention to objects and image regions that are more relevant to the target.

For the object attention redistribution, the object-target association score of each object q is multiplied with the object features S_t to generate the final object embedding \hat{S}_t :

$$\hat{S}_t^q = S_t^q G_t^q \quad q = 1, 2, \dots, N \quad (1)$$

where $\hat{S}_t = \{\hat{S}_t^1, \hat{S}_t^2, \dots, \hat{S}_t^N\}$, N is the number of objects.

For the image attention redistribution, we assign attention to the image features I_t with the help of object semantic embeddings which are generated from the one-hot encodings. Initially, the semantic embeddings are weighted by $G_t \in \mathbb{R}^{N \times 1}$ to obtain the attention-aware object semantics D . We use D as the query and I_t as the key and value in the multi-head image attention to generate the final image embedding \hat{I}_t :

$$Q_i = DW_i^Q \quad K_i = I_t W_i^K \quad V_i = I_t W_i^V \quad i = 1, \dots, NH \quad (2)$$

$$head_i = softmax\left(\frac{Q_i K_i^T}{\sqrt{HD}}\right) V_i \quad (3)$$

$$\hat{I}_t = Concat(head_1, \dots, head_{NH}) W^O \quad (4)$$

where HD and NH denote the hidden dimensionality and number of heads in the multi-head attention.

Finally, the attention-aware object features \hat{S}_t and image features \hat{I}_t are concatenated with the previous action embedding PA to get the output ST of the search thinking network.

Navigation Thinking Network

Target-Oriented Memory Graph (TOMG) Different from the search thinking, the navigation thinking requires the ability to memorize, locate and navigate to the target. Thus, we individually design a target-oriented memory graph (TOMG) as the input feature M . As shown in Figure 2, TOMG is composed of visited target-visible nodes. Each node feature $m \in \mathbb{R}^{1 \times 9}$ is concatenated by three parts: the target bounding box, the target confidence and the agent’s state (position and angle). This target-oriented and thin way of storing visited nodes information brings

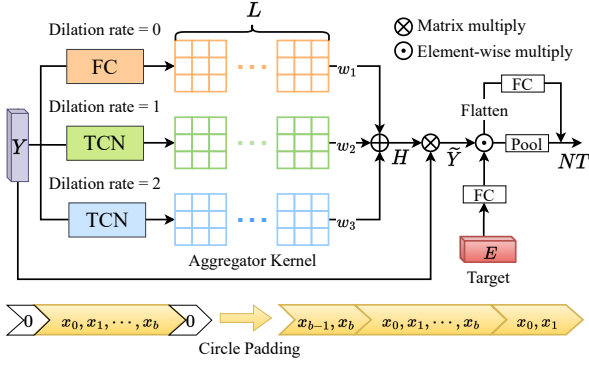


Figure 3: A detailed explanation of the target-aware multi-scale aggregator (TAMSA). We first use the multi-scale TCNs to obtain the aggregator kernels which aggregate the target-oriented memory graph of L nodes into 3 nodes. Then, the aggregated features are allocated attention to the channel dimension using target semantics. We describe the circle padding method in our TCN below the figure.

up to $400\times$ less storage cost compared to previous works (Fukushima et al. 2022; Zhu et al. 2021). Since the agent cannot obtain its own absolute position and orientation in an unknown environment, the stored coordinates take the starting position as the origin and the starting orientation as the coordinate axis. We filter target-visible nodes using a confidence threshold cf . Finally, to reduce the redundancy of storage, only the L closest target-visible nodes to the current node in path are stored. If the number of target-visible nodes is less than L , the remaining nodes are filled with all 0.

Egocentric Coordinate Transformation In above section we mention that the agent’s position (x_i, y_i) and angle (θ_i, β_i) are calculated relative to the starting position (x_0, y_0) and angle (θ_0, β_0) . However, as the agent navigates each step, the decisions (e.g. rotate right) are made relative to its own coordinate system. Therefore, as shown in Figure 2, we convert the coordinates of each node in TOMG to relative to the current node $(x_c, y_c, \theta_c, \beta_c)$ at each step:

$$\begin{aligned} (\tilde{x}_i, \tilde{y}_i) &= (x_i, y_i) - (x_c, y_c) \\ (\tilde{\theta}_i^x, \tilde{\beta}_i^x) &= \sin((\theta_i, \beta_i) - (\theta_c, \beta_c)) \\ (\tilde{\theta}_i^y, \tilde{\beta}_i^y) &= \cos((\theta_i, \beta_i) - (\theta_c, \beta_c)) \quad i \in \Delta_M \end{aligned} \quad (5)$$

where Δ_M represents the index collection of target-visible nodes. In order to make the angle coordinates and the position coordinates in the same order of magnitude, we use \sin and \cos to normalize the angle coordinates to $[-1, 1]$. After the egocentric coordinate transformation, we get the egocentric TOMG features $\tilde{M} \in \mathbb{R}^{L \times 11}$.

Target-Aware Multi-Scale Aggregator (TAMSA) In order to encode the navigation thinking into the network, we design a target-aware multi-scale aggregator (TAMSA) to aggregate the egocentric TOMG feature \tilde{M} into an implicit representation NT . Different from the typical methods that

use transformer or temporal convolution as encoders, we further devise a unique dynamic encoder that can better leverage the memory graph features, as described below.

First, to improve the feature expression ability of the navigate thinking, we use fully connected (FC) layers to map features \tilde{M} into a higher dimensional space. Inspired by some advanced works (Dosovitskiy et al. 2021; Liu et al. 2021) in vision transformer, we add layer normalization between the two FC layers to stabilize the forward input distribution and the gradient of back propagation (Xu et al. 2019). The encoding details can be formulated as follows:

$$Y = \delta(LN(\tilde{M}W^{M_1})W^{M_2}) \quad (6)$$

where δ denotes ReLU function, LN denotes layer normalization, $W^{M_1} \in \mathbb{R}^{11 \times 16}$ and $W^{M_2} \in \mathbb{R}^{16 \times 32}$ are learnable parameters.

Afterwards, a multi-scale dynamic kernel is calculated to refine the target orientation features into the implicit nodes. As shown in Figure 3, we use three temporal convolution networks (TCNs) with different dilation rates d to generate three dynamic kernels with different scales, respectively. It is worth noting that TCN with $d = 0$ degenerates to FC. In the early stage of the "navigate to" phase, the valid nodes in TOMG are fewer, so the boundary degradation caused by zero padding have a greater impact. Accordingly, inspired by (Zhang, Hu, and Wang 2022), we design the circle padding (CP) which fills the sequence edge with the features at the other end of the sequence (Figure 3). The kernels of the three scales are added together after multiplying a learnable parameter w_d :

$$H(l) = \sum_{d=0}^2 w_d \left(\sum_{j \in \Psi} Y(l + j * d) * f_d(j) + b_d \right) \quad (7)$$

where $H = \{H(1), \dots, H(L)\}$, l is the central node of the convolution kernel, Ψ refers to the set of offsets in the neighborhood considering convolution conducted on the center node, $Y(\cdot)$ takes out the node features in Y , f_d and b_d denote the weights and biases in the convolution kernel with dilation rate is d . The multi-scale dynamic kernel $H \in \mathbb{R}^{L \times \mathcal{L}}$ refines $Y \in \mathbb{R}^{L \times 32}$ to $\hat{Y} \in \mathbb{R}^{\mathcal{L} \times 32}$.

Intuitively, the mapping between observation data and target azimuth is different while looking for different targets. For example, when looking for a TV, even if the TV is far away from the agent, the agent can clearly identify the target and get a larger target bounding box, but when looking for a mobile phone, the agent can only get a smaller target bounding box even if it is close enough to the mobile phone. Therefore, we enhance the TAMSA representation by taking the target semantic information into consideration. To achieve this goal, the one-hot target index E is encoded to the same channel dimension as \hat{Y} through two FC layers, whose result is channel-wise multiplied with \hat{Y} to get the target-aware feature representation \hat{Y} :

$$\hat{Y} = H^T Y \odot \delta(\delta(EW^{E_1})W^{E_2}) \quad (8)$$

Finally, to get the final output NT of the navigation thinking network, we flatten \hat{Y} from $\mathbb{R}^{\mathcal{L} \times 32}$ to $\mathbb{R}^{1 \times 32\mathcal{L}}$, and use

a FC layer to reduce the output dimension. Meanwhile, we add residual connections to ensure the stability of feature transfer.

$$NT = \delta(\text{Flatten}(\widehat{Y})W^Y) + \frac{1}{\mathcal{L}} \sum_{l=1}^{\mathcal{L}} \widehat{Y}(l) \quad (9)$$

A dropout layer is added before the output to reduce the overfitting of the navigation thinking network.

Adaptive Fusion (AF) of Dual Thinking Networks

The search thinking and the navigation thinking work together according to the navigation progress. In the “search for” phase, since there is no visited target-visible node, NT is an all-zero matrix. Therefore, the navigation thinking network does not affect the action decision when the target has never been seen. In the “navigate to” phase, to ensure the navigation robustness, search thinking and navigation thinking together guide the action decision. As the number of visited target-visible nodes increases, the influence of navigation thinking is gradually emerging. The fusion process of the two kinds of thinking can be expressed as:

$$DT = (\text{LN}(\text{Concat}(NT, ST)))W \quad (10)$$

where W is the learnable parameter to adaptively adjust the proportion of two thinking networks, and LN is demonstrated to be significantly beneficial to the model generalization.

Policy Learning

Following the setups of the previous works (Mirowski et al. 2017; Fang et al. 2021), we treat this task as a reinforcement learning problem and utilize the asynchronous advantage actor-critic (A3C) algorithm (Mnih et al. 2016). However, in the search thinking network, complex multi-head attention calculations are proved to be difficult to directly learn by the reinforcement learning (Du, Yu, and Zheng 2021), so we use the imitation learning to pre-train the search thinking network in advance. We divide the continuous action process into step-by-step action predictions, and teach the agent only rely on object associations to determine actions without historical navigation information. Through pre-training, we get a search thinking network with basic object association ability. Afterwards, the search thinking network and navigation thinking network are trained jointly by the reinforcement learning to learn an LSTM action policy $\pi(a_t|ST_t, NT_t)$. In accordance with the done reminder operation presented in (Zhang et al. 2021), when the agent detects the target, we use the target detection confidence to explicitly enhance the probability of the *Done* action in the action domain $A_t \in \mathbb{R}^{1 \times 6}$.

Experiment

Experimental Setup

Dataset AI2-Thor (Kolve et al. 2017) is our main experimental platform, which includes 30 different floorplans for each of 4 room layouts: kitchen, living room, bedroom, and

bathroom. For each scene type, we use 20 rooms for training, 5 rooms for validation, and 5 rooms for testing. Agents can only be located at the intersection of 0.25m grids in each room. The camera rotates 45 degrees in the horizontal direction and 30 degrees in the vertical direction each step.

Evaluation Metrics We use the success rate (SR), success weighted by path length (SPL) (Anderson et al. 2018a), and our proposed success weighted by navigation efficiency (SNE) metrics to evaluate our method. SR indicates the success rate in completing tasks, which is formulated as $SR = \frac{1}{F} \sum_{i=1}^F Suc_i$, where F is the number of episodes and Suc_i indicates whether the i -th episode succeeds. SPL considers the path length more comprehensively and is defined as $SPL = \frac{1}{F} \sum_{i=1}^F Suc_i \frac{\mathbb{L}_i^*}{\max(\mathbb{L}_i, \mathbb{L}_i^*)}$, where \mathbb{L}_i is the path length taken by the agent and \mathbb{L}_i^* is the theoretical shortest path. SNE considers the navigation efficiency in the “navigate to” phase and is defined as

$$SNE = \frac{1}{F} \sum_{i=1}^F Suc_i \frac{\mathbb{L}_i}{\mathbb{L}_i^{nav} + 1} \quad (11)$$

where \mathbb{L}_i^{nav} is the path length in the “navigate to” phase. In order to prevent the denominator from being 0, we use $\mathbb{L}_i^{nav} + 1$ as the denominator.

Implementation Details We train our model with 18 workers on 2 RTX 2080Ti Nvidia GPUs. The dropout rate and target-visible filter cf in our model are set to 0.3 and 0.4. The number of implicit nodes \mathcal{L} in TAMSA is 3. We adopt DETR as the object detector and fine-tune DETR on the AI2-Thor training dataset (Du, Yu, and Zheng 2021). We report the results for all targets (ALL) and for a subset of targets ($\mathbb{L} \geq 5$) with optimal trajectory lengths greater than 5.

Ablation Experiments

Baseline Similar to (Dang et al. 2022), our baseline model adopts the features concatenated from image branch (from ResNet18), object branch (from DETR) and previous action branch as the environment perception encoding. Afterwards, LSTM is used to model the temporal implicit features. Finally, the A3C reinforcement learning method allows the agent to learn how to decide the next action. The first row in Table 1 shows the performance of our baseline on various metrics. It is worth noting that since we adopt the object features extracted by DETR, the capabilities of our baseline model are already close to some SOTA methods with FasterRCNN (Ren et al. 2015).

Dual Adaptive Thinking The purpose of dual adaptive thinking is to dynamically use two distinct thinking ways, so that the agent can perform well at every stage. As shown in Table 1, the model with the search thinking outperforms the baseline with the gains of 4.56/7.64, 1.57/2.25 and -0.38/0.69 in SR, SPL and SNE (ALL/ $\mathbb{L} \geq 5$, %). Obviously, the search thinking enables the agent to quickly find the object through object association, but due to lack of estimating the target relative position, SPL is restricted by redundant paths in “navigate to” phase. Adaptively incorporat-

Table 1: Ablation results of each module in the three sub-networks: search, navigate and fusion.

ID	Search Thinking		Navigation Thinking			Fusion		ALL (%)			$\mathbb{L} \geq 5$ (%)		
	Associate	Pretrain	TOMG	Egocentric	TAMSA	AF	LN	SR	SPL	SNE	SR	SPL	SNE
1								71.34	43.47	121.91	60.72	42.18	110.73
2	✓							74.89	44.98	122.32	67.12	44.01	111.81
3	✓	✓						75.90	45.04	121.53	68.36	44.43	111.42
4	✓	✓	✓					76.02	43.15	126.15	68.66	42.19	119.22
5	✓	✓	✓	✓				78.12	42.01	129.12	70.52	41.23	121.87
6	✓	✓	✓		✓			78.04	45.67	131.24	70.34	45.30	125.98
7	✓	✓	✓	✓	✓			80.88	45.71	135.44	73.42	45.91	133.11
8	✓	✓	✓	✓	✓	✓		81.34	47.53	138.12	74.89	47.76	132.82
9	✓	✓	✓	✓	✓	✓	✓	82.39	48.93	139.83	76.21	49.32	138.29

Table 2: Ablation experiments of each module in target-aware multi-scale aggregator (TAMSA). Dynamic: dynamic aggregator kernel, TA: target-aware, MS: multi-scale, CP: circle padding.

Method		ALL (%)			$\mathbb{L} \geq 5$ (%)		
		SR	SPL	SNE	SR	SPL	SNE
Average Pooling		79.67	45.14	134.21	73.33	45.21	126.94
Transformer		77.23	43.24	132.83	71.44	42.97	127.11
TCN		78.66	43.41	133.69	74.42	43.91	125.18
TAMSA	A1 Dynamic	80.15	44.26	135.02	71.80	45.33	130.87
	A2 A1+TA	81.20	46.71	136.25	74.17	47.52	134.91
	A3 A1+MS	81.14	47.28	135.22	73.44	48.31	136.49
	A4 A2+MS	81.32	47.41	137.26	75.88	49.36	138.12
	A5 A4+CP	82.39	48.93	139.83	76.21	49.32	138.29

ing our proposed navigation thinking into the search thinking can improve 6.49/7.85, 3.89/4.89 and 18.3/26.87 in SR, SPL and SNE (ALL/ $\mathbb{L} \geq 5$, %). The results prove that the navigation thinking can improve the agent’s performance on various indicators by optimizing the path of the “navigate to” phase. It can be found from the last two rows in Table 1 that the fusion of dual thinking is considerable for the final model effect.

Navigation Thinking Network The navigation thinking network mainly includes three modules: target-oriented memory graph (TOMG), egocentric coordinate transformation module and target-aware multi-scale aggregator (TAMSA). Rows 4 to 7 in Table 1 show the ablation results on the three modules. The navigation thinking without TAMSA increases SR and SNE by 2.22/2.16 and 7.59/10.45, but decreases SPL by 3.03/3.2 (ALL/ $\mathbb{L} \geq 5$, %). The fundamental reason is that if TAMSA and adaptive fusion are not used, the introduction of navigation thinking is relatively coarse, which will seriously affect the learning of search thinking, reducing the searching ability of the model in the “search for” phase. Although the use of TOMG alone cannot directly improve various indicators, the simplified and highly abstract storage features in TOMG facilitate the subsequent feature refinement and thinking integration. As shown in Figure 4, we display various metrics and computation speed while using different storage features (TOMG, object, image) and maximum stored steps L . Image fea-

tures are the least suitable for navigation thinking and consume the highest computational complexity. The basic reason is that image features are not abstract enough and contain too much redundant information. Compared with object features, the target-oriented characteristic in TOMG brings obvious advantages in SNE. Most importantly, TOMG is far less complex in calculation and memory than other storage methods. In terms of the computational efficiency, when the number of stored steps is 40, TOMG improves the computation speed by 41.43% and 47.69% respectively compared with storing object and image features. In terms of the memory usage, TOMG only needs 0.64% and 0.29% memory compared with storing object and image features. Furthermore, as the number of stored steps increases, using the TOMG storage method hardly increases the computational burden.

Target-Aware Multi-Scale Aggregator (TAMSA) Different from the commonly used encoders such as TCN and transformer, our proposed TAMSA uses dynamic kernel to achieve automatic sequence length reduction without using the global pooling at the end. As shown in Table 2, using either TCN or transformer performs worse than using average pooling directly. The results indicate that these commonly used encoders are not suitable for our navigation thinking. On the initial aggregator model (A1), the target-aware (TA) property brings improvements of 1.05/2.37, 2.45/2.19, 1.23/4.04, and the multi-scale (MS) property brings improvements of 0.99/1.64, 3.02/2.98, 0.20 /5.62 in SR, SPL and SNE (ALL/ $\mathbb{L} \geq 5$, %). The two properties optimize the agent’s route in the “navigate to” phase during long-distance navigation, but have little effect on short-distance navigation. To solve this problem, we utilize the circle padding (CP) to avoid serious information loss with limited target-visible nodes, thereby optimizing the path in short-distance navigation.

Fusion of Dual Thinking modules When humans complete a task, multiple thinking ways often cooperate with each other, rather than work independently. Therefore, how to effectively integrate the two separately designed thinking in the unified network is crucial. From rows 4 to 7 in Table 1, it can be found that after simply adding the navigation thinking, the improvement of SPL is not obvious compared with SNE. The gap suggests that though the naviga-

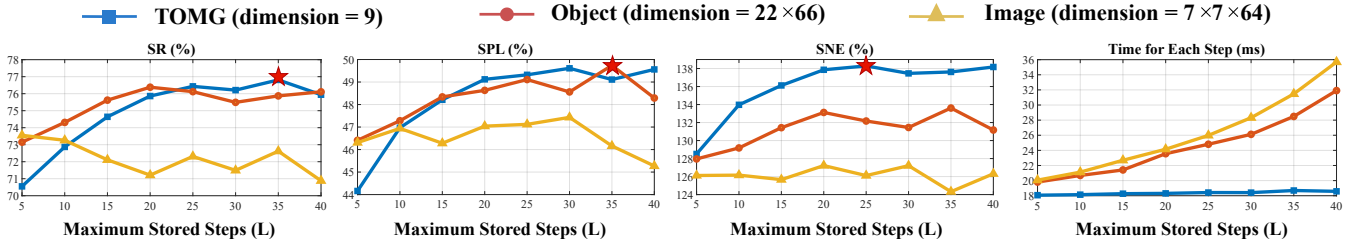


Figure 4: We compare the metrics in paths with $\mathbb{L} \geq 5$, while storing different features and path lengths for the navigation thinking. The red five-pointed star indicates the choice that can make the current indicator optimal.

Table 3: Comparison with SOTA methods on the AI2_Thor.

ID	Method	ALL (%)			$\mathbb{L} \geq 5$ (%)		
		SR	SPL	SNE	SR	SPL	SNE
I	Random	4.12	2.21	7.91	0.21	0.08	8.14
	SAVN (2019)	63.12	37.81	102.44	52.01	34.94	94.51
	ORG (2020)	67.32	37.01	111.88	58.13	35.90	101.29
	HOZ (2021)	68.53	37.50	110.79	60.27	36.61	106.37
	VTNet (2021)	72.24	44.57	115.99	63.19	43.84	109.80
	DOA (2022)	74.32	40.27	120.86	67.88	40.36	109.19
II	OMT (2022)	71.13	37.27	124.31	61.94	38.19	117.98
III	SSCNav (2021)	77.14	35.09	138.22	71.73	34.33	136.87
	PONI (2022)	78.58	37.27	141.17	72.92	36.40	137.26
IV	Ours (DAT)	82.39	48.93	139.83	76.21	49.32	138.29

tion thinking optimizes the “navigate to” phase, it has a negative impact on the “search for” phase dominated by search thinking. Our proposed adaptive fusion (AF) method solves the above problem and brings 0.46/1.47 and 1.82/1.85 improvements in SR and SPL (ALL/ $\mathbb{L} \geq 5$, %). Moreover, since the feature modal and encoding methods used by the search thinking and navigation thinking are completely different, directly concatenating the two thinking features will lead to the backpropagation instability and serious overfitting. Therefore, the layer normalization (LN) is used after the concatenation of the two thinking features, which brings the improvements of 1.05/1.32, 1.40/1.56 and 1.71/5.47 in SR, SPL and SNE (ALL/ $\mathbb{L} \geq 5$, %).

Comparisons to the State-of-the-art

Our DAT method is compared with three categories of SOTA methods relevant to ours in Table 3. **(I) Methods with search thinking.** These methods have lower SNE because they do not have the navigation thinking. Compared to the recently proposed DOA (Dang et al. 2022) method, our DAT method brings 8.07/8.33, 8.66/8.96 and 18.97/29.10 improvements in SR, SPL and SNE (ALL/ $\mathbb{L} \geq 5$, %). **(II) Methods with the long-term memory.** These methods can theoretically depend on the historical information to model the environment more clearly, but methods such as OMT (Fukushima et al. 2022) store overcomplicated features, causing the network learning too difficult. Therefore, the current memory modules do not exert their full strength. **(III) Modular methods based on semantic maps.** The strong interpretability of semantic maps enables agents to

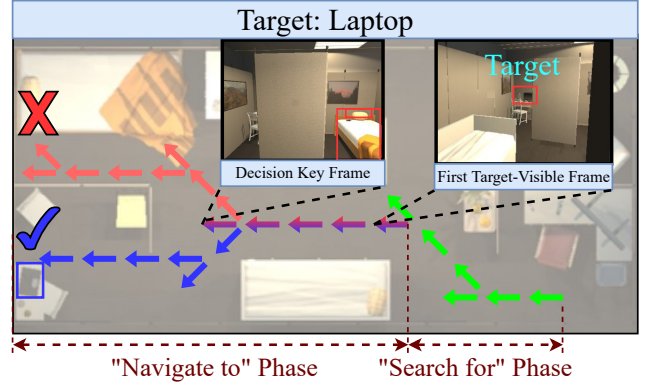


Figure 5: Visualization on the RoboTHOR test environment. Green arrows: “search for” phase; Red arrows: route with only the search thinking in the “navigate to” phase; Blue arrows: route with both the search and navigation thinking in the “navigate to” phase. The both routes differ at the decision key frame.

quickly navigate to the target location after seeing the target, so their “navigate to” phase efficiency (SNE) is higher. Nevertheless, these methods require considerable efforts to explore the environment, resulting in the inability to visually capture objects as quickly as search thinking methods. As described, the current state-of-the-art modular method PONI (Ramakrishnan et al. 2022) is 11.66/12.92 lower in SPL (ALL/ $\mathbb{L} \geq 5$, %) than our DAT method.

Qualitative Analysis

We visualize the route in the environment using only search thinking and our DAT method in Figure 5. In the “search for” phase, the paths predicted by two methods are the same since our DAT has not invoked the proposed navigation thinking network yet. After entering the “navigate to” phase, the navigation thinking of the DAT method begins to assist the agent’s decision-making by structuring the memory graph of the target information. At the decision key frame, the target cannot be seen. The method with only search thinking selects the right room with richer object information. On the contrary, our DAT method uses the target relative position representation generated by the navigation thinking to select the correct left room. The correct decision in this key frame leads to the successful navigation of our DAT method.

Multiple Adaptive Thinking in Embodied AI

The dual adaptive thinking (DAT) network proposed in this paper can bring a universal inspiration to researchers. In the object navigation task, dual adaptive thinking can be extended to multiple adaptive thinking. The environment modeling thinking, object state understanding thinking, etc. are necessary to be introduced into the multiple adaptive thinking model. Furthermore, the multiple adaptive thinking is not limited to object navigation tasks. In other embodied AI tasks, such as embodied question answering (EQA) (Das et al. 2018) and visual language navigation (VLN) (Anderson et al. 2018b), the agent also needs to use multiple thinking to deal with real-world problems more flexibly.

Conclusion

This paper endows the agent dual adaptive thinking (DAT) to solve the problem of not being able to quickly reach the target position after seeing the target. Dual thinking includes the search thinking responsible for searching the target and the navigation thinking responsible for navigating to the target. The extensive experiments prove that dual adaptive thinking can flexibly adjust the thinking way according to the navigation stage, thereby improving the success rate and efficiency of navigation. It is worth noting that beyond the object navigate task, the multiple adaptive thinking is theoretically applicable to other time-series embodied AI tasks.

References

- Anderson, P.; Chang, A.; Chaplot, D. S.; Dosovitskiy, A.; Gupta, S.; Koltun, V.; Kosecka, J.; Malik, J.; Mottaghi, R.; Savva, M.; et al. 2018a. On evaluation of embodied navigation agents. *arXiv preprint arXiv:1807.06757*.
- Anderson, P.; Wu, Q.; Teney, D.; Bruce, J.; Johnson, M.; Sünderhauf, N.; Reid, I.; Gould, S.; and Van Den Hengel, A. 2018b. Vision-and-language navigation: Interpreting visually-grounded navigation instructions in real environments. In *Proceedings of the IEEE conference on computer vision and pattern recognition*, 3674–3683.
- Carion, N.; Massa, F.; Synnaeve, G.; Usunier, N.; Kirillov, A.; and Zagoruyko, S. 2020. End-to-end object detection with transformers. In *European conference on computer vision*, 213–229. Springer.
- Chaplot, D. S.; Gandhi, D. P.; Gupta, A.; and Salakhutdinov, R. R. 2020. Object goal navigation using goal-oriented semantic exploration. *Advances in Neural Information Processing Systems*, 33: 4247–4258.
- Dang, R.; Shi, Z.; Wang, L.; He, Z.; Liu, C.; and Chen, Q. 2022. Unbiased Directed Object Attention Graph for Object Navigation. *arXiv preprint arXiv:2204.04421*.
- Das, A.; Datta, S.; Gkioxari, G.; Lee, S.; Parikh, D.; and Batra, D. 2018. Embodied question answering. In *Proceedings of the IEEE Conference on Computer Vision and Pattern Recognition*, 1–10.
- Dosovitskiy, A.; Beyer, L.; Kolesnikov, A.; Weissenborn, D.; Zhai, X.; Unterthiner, T.; Dehghani, M.; Minderer, M.; Heigold, G.; Gelly, S.; Uszkoreit, J.; and Houshy, N. 2021. An Image is Worth 16x16 Words: Transformers for Image Recognition at Scale. In *9th International Conference on Learning Representations, ICLR 2021, Virtual Event, Austria, May 3-7, 2021*.
- Du, H.; Yu, X.; and Zheng, L. 2020. Learning Object Relation Graph and Tentative Policy for Visual Navigation. In *Computer Vision – ECCV 2020: 16th European Conference, Glasgow, UK, August 23–28, 2020, Proceedings, Part VII*, 19–34.
- Du, H.; Yu, X.; and Zheng, L. 2021. VTNet: Visual transformer network for object goal navigation. *arXiv preprint arXiv:2105.09447*.
- Duan, J.; Yu, S.; Tan, H. L.; Zhu, H.; and Tan, C. 2022. A survey of embodied ai: From simulators to research tasks. *IEEE Transactions on Emerging Topics in Computational Intelligence*.
- Fang, Q.; Xu, X.; Wang, X.; and Zeng, Y. 2021. Target-driven visual navigation in indoor scenes using reinforcement learning and imitation learning. *CAAI Transactions on Intelligence Technology*.
- Fukushima, R.; Ota, K.; Kanazaki, A.; Sasaki, Y.; and Yoshiyasu, Y. 2022. Object Memory Transformer for Object Goal Navigation. *arXiv preprint arXiv:2203.14708*.
- Gao, C.; Chen, J.; Liu, S.; Wang, L.; Zhang, Q.; and Wu, Q. 2021. Room-and-object aware knowledge reasoning for remote embodied referring expression. In *Proceedings of the IEEE/CVF Conference on Computer Vision and Pattern Recognition*, 3064–3073.
- He, K.; Zhang, X.; Ren, S.; and Sun, J. 2016. Deep residual learning for image recognition. In *Proceedings of the IEEE conference on computer vision and pattern recognition*, 770–778.
- Kolve, E.; Mottaghi, R.; Han, W.; VanderBilt, E.; Weihs, L.; Herrasti, A.; Gordon, D.; Zhu, Y.; Gupta, A.; and Farhadi, A. 2017. AI2-THOR: An Interactive 3D Environment for Visual AI. *arXiv*.
- Li, X.; Guo, D.; Liu, H.; and Sun, F. 2022. REVE-CE: Remote Embodied Visual Referring Expression in Continuous Environment. *IEEE Robotics and Automation Letters*, 7(2): 1494–1501.
- Liang, Y.; Chen, B.; and Song, S. 2021. Sscnav: Confidence-aware semantic scene completion for visual semantic navigation. In *2021 IEEE International Conference on Robotics and Automation (ICRA)*, 13194–13200. IEEE.
- Liu, L.; Ouyang, W.; Wang, X.; Fieguth, P.; Chen, J.; Liu, X.; and Pietikäinen, M. 2020. Deep learning for generic object detection: A survey. *International journal of computer vision*, 128(2): 261–318.
- Liu, Z.; Lin, Y.; Cao, Y.; Hu, H.; Wei, Y.; Zhang, Z.; Lin, S.; and Guo, B. 2021. Swin transformer: Hierarchical vision transformer using shifted windows. In *Proceedings of the IEEE/CVF International Conference on Computer Vision*, 10012–10022.
- Mirowski, P.; Pascanu, R.; Viola, F.; Soyer, H.; Ballard, A. J.; Banino, A.; Denil, M.; Goroshin, R.; Sifre, L.; Kavukcuoglu, K.; et al. 2017. Learning to navigate in complex environments. In *5th International Conference on Learning Representations*.

Mnih, V.; Badia, A. P.; Mirza, M.; Graves, A.; Lillicrap, T.; Harley, T.; Silver, D.; and Kavukcuoglu, K. 2016. Asynchronous methods for deep reinforcement learning. In *International conference on machine learning*, 1928–1937. PMLR.

Moghaddam, M. K.; Abbasnejad, E.; Wu, Q.; Shi, J. Q.; and Van Den Hengel, A. 2022. ForeSI: Success-Aware Visual Navigation Agent. In *Proceedings of the IEEE/CVF Winter Conference on Applications of Computer Vision*, 691–700.

Ramakrishnan, S. K.; Chaplot, D. S.; Al-Halah, Z.; Malik, J.; and Grauman, K. 2022. PONI: Potential Functions for ObjectGoal Navigation with Interaction-free Learning. In *Proceedings of the IEEE/CVF Conference on Computer Vision and Pattern Recognition*, 18890–18900.

Ren, S.; He, K.; Girshick, R.; and Sun, J. 2015. Faster r-cnn: Towards real-time object detection with region proposal networks. *Advances in neural information processing systems*, 28.

Shridhar, M.; Thomason, J.; Gordon, D.; Bisk, Y.; Han, W.; Mottaghi, R.; Zettlemoyer, L.; and Fox, D. 2020. Alfred: A benchmark for interpreting grounded instructions for everyday tasks. In *Proceedings of the IEEE/CVF conference on computer vision and pattern recognition*, 10740–10749.

Wang, W.; Yang, Y.; Wang, X.; Wang, W.; and Li, J. 2019. Development of convolutional neural network and its application in image classification: a survey. *Optical Engineering*, 58(4): 040901.

Wortsman, M.; Ehsani, K.; Rastegari, M.; Farhadi, A.; and Mottaghi, R. 2019. Learning to learn how to learn: Self-adaptive visual navigation using meta-learning. In *Proceedings of the IEEE/CVF Conference on Computer Vision and Pattern Recognition*, 6750–6759.

Xu, J.; Sun, X.; Zhang, Z.; Zhao, G.; and Lin, J. 2019. Understanding and improving layer normalization. *Advances in Neural Information Processing Systems*, 32.

Yang, W.; Wang, X.; Farhadi, A.; Gupta, A.; and Mottaghi, R. 2019. Visual Semantic Navigation using Scene Priors. In *7th International Conference on Learning Representations, ICLR 2019, New Orleans, LA, USA, May 6-9, 2019*.

Zhang, H.; Hu, W.; and Wang, X. 2022. EdgeFormer: Improving Light-weight ConvNets by Learning from Vision Transformers. *arXiv preprint arXiv:2203.03952*.

Zhang, S.; Song, X.; Bai, Y.; Li, W.; Chu, Y.; and Jiang, S. 2021. Hierarchical Object-to-Zone Graph for Object Navigation. In *Proceedings of the IEEE/CVF International Conference on Computer Vision*, 15130–15140.

Zhu, C.; Meurer, M.; and Günther, C. 2022. Integrity of Visual Navigation—Developments, Challenges, and Prospects. *NAVIGATION: Journal of the Institute of Navigation*, 69(2).

Zhu, F.; Liang, X.; Zhu, Y.; Yu, Q.; Chang, X.; and Liang, X. 2021. SOON: scenario oriented object navigation with graph-based exploration. In *Proceedings of the IEEE/CVF Conference on Computer Vision and Pattern Recognition*, 12689–12699.